

Generating Robust Optical Entanglement in Weak Coupling Optomechanical Systems

Mark C. Kuzyk,* Steven J. van Enk, and Hailin Wang

Department of Physics and Oregon Center for Optics, University of Oregon, Eugene, OR 97403, USA

(Dated: September 4, 2018)

A pulsed scheme for generating robust optical entanglement via the coupling of two optical modes to a mechanical oscillator is proposed. This scheme is inspired by the Sørensen-Mølmer approach for entangling trapped ions in a thermal environment and is based on the use of optical driving pulses that are slightly detuned from the respective sideband resonance. We show that for certain pulse durations, the optomechanical interaction can return the mechanical oscillator to its initial state. The corresponding entanglement generation is robust against thermal mechanical noise in the weak as well as the strong coupling regimes. Significant optical entanglement can be generated in the weak coupling regime, even in the presence of a large thermal phonon occupation.

Introduction- In an optomechanical resonator, a mechanical oscillator can interact with any of the optical modes via radiation pressure. This property can enable a quantum interface that converts photons between vastly different wavelengths or couple together different types of quantum systems in a hybrid quantum network [1–11]. A multi-mode optomechanical system also provides an experimental platform for generating continuous variable quantum entanglement of optical modes through the formation of Bogoliubov optical modes, and in particular, for generating entanglement between optical and microwave modes [12–15].

Entanglement generation is often hampered by dissipation and decoherence induced by the unavoidable coupling to the environment. For generation of optical entanglement via an optomechanical process, a major obstacle is the coupling of the mechanical oscillator to the thermal reservoir. A recently proposed scheme has exploited the coherent dynamics of the Bogoliubov modes to circumvent thermal mechanical noise [13]. The thermal robustness of the Bogoliubov-mode based schemes hinges on the achievement of very strong optomechanical coupling, for which the effective multi-photon optomechanical coupling rate far exceeds the damping rates of the relevant optical and mechanical modes. Although strong coupling has been achieved for individual optomechanical systems in both optical and microwave regimes [16–18], it is exceedingly difficult to have the optomechanical coupling rate to be much greater than the cavity decay rate in the optical regime, especially in a setting that is suitable for generating entanglement between optical and microwave modes.

In this letter, we propose and analyze an optomechanical scheme for optical entanglement generation, which takes advantage of a special class of multi-mode interaction Hamiltonian, instead of Bogoliubov modes, to circumvent thermal mechanical noise. This scheme is inspired by earlier theoretical and experimental studies on entangling trapped ions in a thermal environment [19–21]. In these studies, the entanglement operation takes place via the mechanical degrees of freedom of the ions. As shown by Sørensen and Mølmer, robust entanglement

can be achieved in a thermal environment with a class of Hamiltonian that returns the motion of the ions to their initial state upon the completion of the entanglement operation [20, 21]. Here, we outline a pulsed entanglement scheme using an optomechanical interaction Hamiltonian that has the features of the Sørensen-Mølmer (S-M) mechanism. The entanglement scheme, which will be referred to as the Sørensen-Mølmer scheme, can function in the weak as well as strong coupling regime. In comparison with the Bogoliubov-mode based schemes, the Sørensen-Mølmer scheme can remain robust against the thermal mechanical noise even in the weak coupling regime. Our theoretical analysis shows that significant optical entanglement can be generated in the weak coupling regime, even in the presence of a large thermal phonon occupation ($n_{th} \sim 1000$).

Three-mode optomechanical system- We consider an optomechanical system, in which two optical modes with resonance frequencies $\omega_{c,i}$ ($i = 1, 2$) and cavity linewidths κ_i , couple to a mechanical oscillator of frequency ω_m and mechanical linewidth γ (see Fig. 1a). The optomechanical coupling is driven by strong laser fields of frequency $\omega_{L,i}$ near the mechanical sideband of the respective cavity resonance. This type of three-mode optomechanical systems has already been used for the experimental demonstration of optomechanics-based optical wavelength conversion [8–10] and for the realization of an optomechanical dark mode [8, 22]. In a frame where each optical mode rotates at its driving frequency $\omega_{L,i}$, and after the standard linearization process, the effective Hamiltonian of the system is

$$H = \omega_m b^\dagger b + \sum_{i=1}^2 \left(\Delta_i a_i^\dagger a + g_i (a_i + a_i^\dagger) (b + b^\dagger) \right), \quad (1)$$

where b and a_i are the annihilation operators for the mechanical and optical modes, respectively, and $\Delta_i = \omega_{c,i} - \omega_{L,i}$ is the detuning of the driving field from the respective cavity resonance. The effective coupling rate g_i is controlled by the strength of the driving field according to $g_i = \sqrt{N_i} g_{0,i}$, where N_i is the intra-cavity photon number for the driving field and $g_{0,i}$ is the single-photon optomechanical coupling rate.

The linearized interaction Hamiltonian couples each optical mode to the mechanical oscillator with two types of interaction. A beam-splitter interaction, associated with the term $g_i(a_i^\dagger b + a_i b^\dagger)$, is an anti-Stokes scattering process that can enable state transfer between optical and the mechanical systems. A two-mode squeezing interaction, of the form $g_i(a_i b + a_i^\dagger b^\dagger)$, is a Stokes scattering process that generates correlated phonon-photon pairs. The beam-splitter interaction has been used for the experimental realization of coherent inter-conversion between optical and mechanical excitations [18, 23, 24] as well as the optomechanically-induced transparency [17, 25, 26] and has also been exploited for optical wavelength conversion in the three-mode optomechanical system. The two-mode squeezing interaction has been employed in earlier theoretical proposals for generating continuous variable entanglement between optical and mechanical modes and also between two mechanical modes [27–32].

For the generation of two-mode optical entanglement, mode 1 is driven near the red sideband, at frequency $\omega_{L,1} = \omega_{c,1} - \omega_m - \Delta$, while mode 2 is driven near the blue sideband, at frequency $\omega_{L,2} = \omega_{c,2} + \omega_m + \Delta$, where Δ is the detuning from the sideband resonance, as illustrated schematically in Fig. 1b. The optomechanical system is assumed to be in the resolved sideband limit, with $\omega_m \gg \kappa_{1,2} \gg \gamma$, such that a driving field near the red sideband or blue sideband drives either the beam-splitter or two-mode squeezing interaction, respectively. Heuristically, entanglement between modes 1 and 2 in this system is generated in two steps. The two-mode squeezing interaction driven by the laser field near the blue sideband generates entanglement between phonons in the mechanical oscillator and photons in mode 2. The beam-splitter interaction driven by the laser field near the red sideband then maps the state of the entangled phonons onto photons in mode 1.

Sørensen-Mølmer Mechanism- To gain insights into the dynamics of the coherent optomechanical interactions and to discuss the S-M mechanism for the three-mode optomechanical system, we first ignore the damping of both optical and mechanical systems and adjust the optomechanical coupling rates for the two optical modes such that $g_1 = g_2 = g$. In this limit, the interaction Hamiltonian for the entanglement generation falls into a class discussed originally by Mølmer and Sørensen and also by Milburn [19, 21, 33]. For this class, the exact propagator can be written in a form

$$U(t) = e^{-iA(x,p,t)} e^{-iF(x,p,t)x_b} e^{-iG(x,p,t)p_b}, \quad (2)$$

where $x = x_1 + x_2$ and $p = p_2 - p_1$ are EPR-like variables, with the dimensionless quadrature variables defined as $x_i = (a_i + a_i^\dagger)/\sqrt{2}$, $p_i = i(a_i^\dagger - a_i)/\sqrt{2}$, and similarly for the mechanical mode operators x_b and p_b . At regularly

spaced time intervals $t_n = 2\pi n/\Delta$,

$$F(x, p, t_n) = G(x, p, t_n) = 0, \quad (3)$$

returning the mechanical degrees of freedom to their initial states. At the same time, $A(x, p, t_n)$, which is given by,

$$A(x, p, t_n) = -\frac{g^2}{2\Delta}(x^2 + p^2)t_n \quad (4)$$

generates entanglement between modes 1 and 2, according to

$$U^\dagger(x, p, t_n) a_{1(2)} U(x, p, t_n) = \mu a_{1(2)} + \nu a_{2(1)}^\dagger, \quad (5)$$

where $\mu = 1 + ir$ and $\nu = ir$, with a squeezing parameter $r = g^2 t_n / 2\Delta$ (see the supplementary materials for the derivation of the propagator and for the analytical expression of the entanglement).

It is remarkable that independent of the particular form of the initial state of the system, the mechanical oscillator periodically returns to its initial state, and leaves the optical modes increasingly entangled upon each return. The entanglement is generated through the mechanical motion of the system. However, the final entangled optical state contains no information of the mechanical system, and can thus be robust against thermal Brownian noise that enters the system through the mechanical oscillator. Note that in the limit of large detuning Δ , the mechanical degrees of freedom can be adiabatically eliminated. The optical entanglement generation can thus become thermally robust without satisfying the condition, $t_n = 2\pi n/\Delta$. The large detuning, however, limits the amplitude of the squeezing parameter and hence the degree of entanglement that can be achieved.

Analysis with Langevin equations- We have used the quantum Langevin equations to analyze in detail the dynamics of the entanglement generation and especially the effects of thermal mechanical noise. We work in a rotating frame $\tilde{H} = U_R H U_R^\dagger$, where H is the Hamiltonian of Eq. (1), and $U_R = e^{i(\omega_m + \Delta)(a_1^\dagger a_1 - a_2^\dagger a_2 + b^\dagger b)t}$. In this frame, the quantum Langevin equations in the resolved sideband limit have the form

$$\dot{a}_1 = -\frac{\kappa_1}{2} a_1 - ig_1 b - \sqrt{\kappa_1} a_{in,1} \quad (6)$$

$$\dot{a}_2^\dagger = -\frac{\kappa_2}{2} a_2^\dagger + ig_2 b - \sqrt{\kappa_2} a_{in,2}^\dagger \quad (7)$$

$$\dot{b} = -(i\Delta + \frac{\gamma}{2})b - ig_1 a_1 - ig_2 a_2^\dagger - \sqrt{\gamma} b_{in}, \quad (8)$$

where the resolved sideband limit has allowed us to drop all counter-rotating terms. The input operators for the optical modes, $a_{in,i}(t)$, characterize the optical cavity coupling to the vacuum, and have correlation functions $\langle a_{in,i}(t) a_{in,i}^\dagger(t') \rangle = \delta(t - t')$. The Brownian noise that enters the system through the mechanical degree

of freedom is described by the operator $b_{in}(t)$. We assume the system to have a sufficiently large mechanical quality factor $Q_m = \omega_m/\gamma$ such that the Brownian noise can be approximated to be Markovian [34], with $\langle b_{in}(t)b_{in}^\dagger(t') \rangle = (n_{th} + 1)\delta(t - t')$.

The entanglement is generated for optical driving pulses with a given duration and is quantified with the logarithmic negativity, $E_{\mathcal{N}}$ [35, 36]. We limit the duration of the optical pulse to ensure that the optomechanical system remains dynamically stable and that nonlinear optomechanical interactions are negligible. For typical optomechanical systems, the mechanical damping rate can be much smaller than both the cavity linewidth and the effective optomechanical coupling rate. To generate strong entanglement and maintain thermal robustness, we have used sideband detuning that is less than g , but far exceeds γ . In the following, we first consider the intracavity entanglement in the strong coupling regime, where $g \gg \kappa_i$. We then analyze the entanglement contained in an output mode for a system in the bad cavity limit with $g \ll \kappa_i$.

Strong coupling- Figure 2a plots the intracavity entanglement generated in the strong coupling regime. As shown in Fig. 2a, the negativity oscillates as a function of time, with the peaks or the maxima of the negativity located at times t_n , when the mechanical degree of freedom is returned to its initial state, as anticipated from the above theoretical treatment without the inclusion of the damping processes. With increasing thermal phonon occupation, the maxima decrease gradually, but the oscillation becomes much more pronounced, with the minima in the negativity quickly approaching zero, illustrating the importance and also the effectiveness of the S-M mechanism in circumventing the thermal mechanical noise.

For comparison, Fig. 2b plots the intracavity entanglement as a function of time, generated in the same system and under otherwise similar conditions by the method of the Bogoliubov mode [13]. In this case, the entanglement maxima occur when the mechanical oscillator returns to its initial state through the Rabi oscillation of the bright Bogoliubov modes that couple to the mechanical oscillator. The period of the oscillation in the negativity in Fig. 2b is thus determined by the effective optomechanical

coupling rate of the bright modes. At very low thermal phonon occupation, the Bogoliubov mode approach can generate stronger maximum entanglement. However, the entanglement is much more sensitive to the timing of the optical field than that generated with the S-M mechanism (see Fig. 2). A small deviation from an exact optomechanical π pulse leads to appreciable mixing between the optical and mechanical excitations.

For a more detailed comparison of the thermal robustness of the two entanglement schemes, we plot in Fig. 3 the maximum negativity obtained under the conditions of Fig. 2 for each entanglement scheme as a function of the initial thermal phonon occupation. As shown in Fig. 3, the Sørensen-Mølmer scheme becomes advantageous when n_{th} exceeds 500, which further highlights the robustness of the Sørensen-Mølmer scheme against thermal mechanical noise. Because of the detuning from the sideband resonance, the S-M mechanism is more effective in returning the mechanical oscillator to its initial state than the coherent dynamics of the Bogoliubov bright modes and thus is more robust against thermal mechanical noise.

Bad cavity limit- In the bad cavity limit, we solve the optical modes adiabatically and investigate the entanglement in the output of the cavity as a function of pulse duration. The entanglement in the cavity output is more relevant to experimental implementation and to potential applications than the intracavity entanglement. Starting with Eq. (6), the adiabatic solutions for the optical modes are

$$a_1(t) = -\frac{2ig_1}{\kappa_1}b(t) - \frac{2}{\sqrt{\kappa_1}}a_{in,1}(t) \quad (9)$$

$$a_2^\dagger(t) = \frac{2ig_2}{\kappa_2}b(t) - \frac{2}{\kappa_2}a_{in,2}^\dagger(t), \quad (10)$$

where $b(t)$ is the formal solution of the mechanical mode. Using the input-output relation $a_{out} = a_{in} + \sqrt{\kappa}a$, the cavity output is related to the input by

$$a_{out,1}(t) = -2i\sqrt{G_1}b(t) - a_{in,1}(t) \quad (11)$$

$$a_{out,2}^\dagger(t) = 2i\sqrt{G_2}b(t) - a_{in,2}^\dagger(t), \quad (12)$$

where

$$b(t) = b(0)e^{-zt} + e^{-zt} \int_0^t e^{zs} \left(2i\sqrt{G_1}a_{in,1}(s) + 2i\sqrt{G_2}a_{in,2}^\dagger(s) - \sqrt{\gamma}b_{in}(s) \right) ds. \quad (13)$$

The complex number $z = \Gamma + i\Delta$ contains an effective damping rate $\Gamma = 2G_1 - 2G_2 + \gamma/2$, where the coupling rates $G_i = g_i^2/\kappa_i$ effectively characterize the optomechanical interaction strength in the bad cavity limit. This also

leads to a modified requirement for the S-M mechanism, $G_1 = G_2$.

The output modes $a_{out,i}(t)$ are improper continuous operators, not well suited for characterizing entangle-

ment. One may instead describe the system in a discrete mode basis by defining independent discrete bosonic operators [37]

$$A_{out,i}^{(k)} = \int dt \phi_k^*(t) a_{out,i}(t) \quad (14)$$

where $i = 1, 2$ again label the two optical modes of the system, the index k labels members of a denumerably infinite set, and the mode functions $\phi_k(t)$ form a complete orthonormal basis under the inner product $\int dt \phi_k^*(t) \phi_{k'}(t)$. The operators defined by equation (14) satisfy the proper commutation relations, $[A_{out,i}^{(j)}, A_{out,i}^{(k)\dagger}] = \delta_{jk}$, for characterizing the entanglement of the output modes with logarithmic negativity.

We study the entanglement between two particular discrete modes of the output, defined as

$$A_{out,i} = \frac{1}{\sqrt{\tau}} \int_0^\tau dt a_{out,i}(t). \quad (15)$$

These modes have central frequencies at the cavity resonances $\omega_{c,1}$ and $\omega_{c,2}$, and describe pulses of duration τ . By extracting only one mode from each output field, we have performed a local operation, which can only decrease the total amount of entanglement in the system [38, 39]. Thus, the entanglement we calculate gives a lower bound on the total entanglement of the system.

The S-M mechanism remains effective in the regime of weak optomechanical coupling. Figure 4a plot the entanglement contained in the modes defined by Eq. (15), as a function of the pulse duration τ , and for various thermal phonon occupations. Similar to the results obtained in the strong coupling regime shown in Fig. 2a, we find that the negativity oscillates with the pulse duration, with the entanglement maxima occurring at pulse durations satisfying the condition of $t_n = 2\pi n/\Delta$. With increasing thermal phonon occupation, the maxima decrease gradually, while the minima quickly approach zero. Significant entanglement can be still achieved with a thermal phonon occupation of order 1000.

The S-M mechanism for the three-mode optomechanical system requires equal effective optomechanical coupling for the two optical modes. To illustrate this, we plot in Fig. 4b the negativity as a function of the thermal phonon occupation when the requirement of $G_1 = G_2$ is satisfied (solid), and when the requirement is not (dashed). Thermally robust entanglement can be achieved only when $G_1 = G_2$ is satisfied. Note that with $\Delta = 0$ and in the weak coupling regime, thermally robust entanglement cannot be achieved regardless whether $G_1 = G_2$ is satisfied.

Conclusions- In summary, we have presented a pulsed approach, in which the optical driving fields are slightly detuned from the respective sideband resonance, for generating optical entanglement in a three-mode optomechanical system. In this approach, the mechanical oscillator returns to its initial state and is disentangled

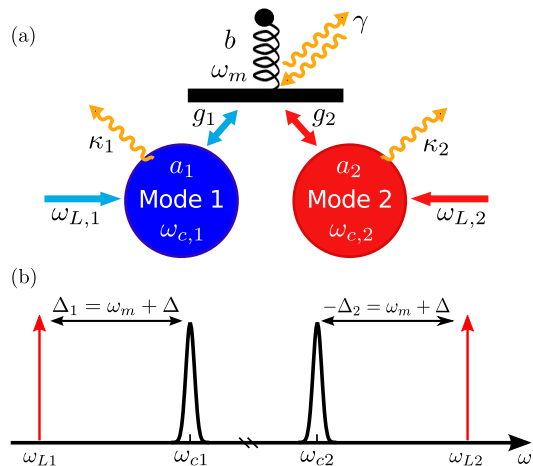


FIG. 1. (a) Schematic of the three-mode optomechanical system. (b) Spectral position of the optical driving fields.

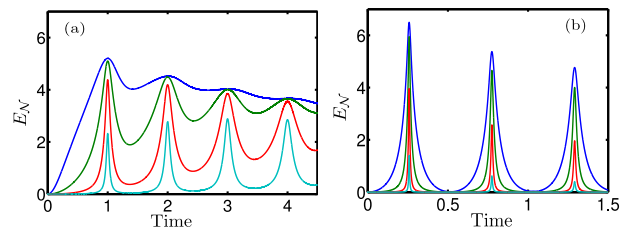


FIG. 2. Intracavity entanglement versus time. (a) Sørensen-Mølmer scheme with $g/\gamma = 4 \cdot 10^3$ and $\Delta/\gamma = 10^3$. (b) Bogoliubov mode scheme with $g_1/\gamma = 4 \cdot 10^3$ and $g_2/\gamma = 3.5 \cdot 10^3$. For both (a) and (b), $\kappa_1/\gamma = \kappa_2/\gamma = 10$ and the time is in units of $2\pi/(10^3\gamma)$. From top to bottom, $n_{th} = 10, 10^2, 10^3, 10^4$.

with the optical modes upon the completion of the entanglement operation. Although schemes based on the use of the Bogoliubov modes can lead to greater entanglement when the mechanical oscillator is near the motional ground state, the Sørensen-Mølmer scheme is more robust against thermal mechanical noise. In particular, significant entanglement can still persist at relatively high thermal phonon occupation in the weak coupling regime, providing a promising avenue for generating optical entanglement, including that between optical and microwave modes.

We would like to thank Lin Tian for helpful discussions and valuable assistances. This work is supported by NSF award No. 1205544 and by the DARPA-MTO ORCHID program through a grant from AFOSR.

* mkuzyk@uoregon.edu

[1] K. Stannigel, P. Rabl, A. S. Sørensen, P. Zoller, and M. D. Lukin, Physical review letters **105**, 220501 (2010)

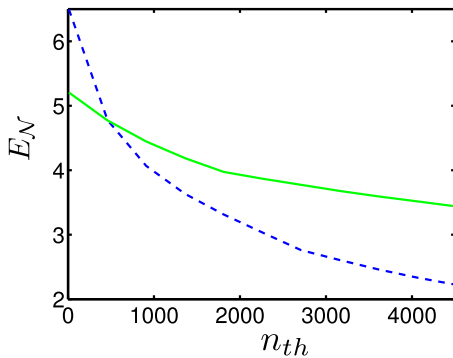


FIG. 3. Maximum intracavity entanglement as a function of thermal phonon occupation n_{th} . The solid (dashed) line is for the Sørensen-Mølmer (Bogoliubov mode) scheme.

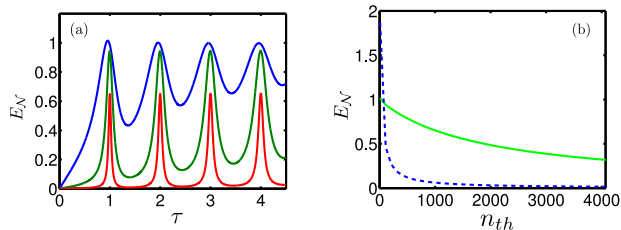


FIG. 4. Entanglement of an output mode in the bad cavity limit, with $\Delta/\gamma = 10^3$ and $\kappa_1/\gamma = \kappa_2/\gamma = 6 \cdot 10^3$. (a) As a function of pulse duration τ , in units of $2\pi/(10^3\gamma)$, with $G_1/\gamma = G_2/\gamma = 667$. From top to bottom, $n_{th} = 10, 10^2, 10^3$. (b) Maximum entanglement generated as a function of thermal phonon occupation. Solid line: $G_1 = G_2$. Dashed line: $G_1/\gamma = 667$ and $G_2/\gamma = 540$.

[2] L. Tian and H. Wang, *Physical Review A* **82**, 053806 (2010)
 [3] A. H. Safavi-Naeini and O. Painter, *New Journal of Physics* **13**, 013017 (2011)
 [4] C. Regal and K. Lehnert, *Journal of Physics: Conference Series* **264**, 012025 (2011)
 [5] Y.-D. Wang and A. A. Clerk, *Physical Review Letters* **108**, 153603 (2012)
 [6] L. Tian, *Physical Review Letters* **108**, 153604 (2012)
 [7] S. Singh, H. Jing, E. Wright, and P. Meystre, *Physical Review A* **86**, 021801 (2012)
 [8] C. Dong, V. Fiore, M. C. Kuzyk, and H. Wang, *Science* **338**, 1609 (2012)
 [9] J. T. Hill, A. H. Safavi-Naeini, J. Chan, and O. Painter, *Nature communications* **3**, 1196 (2012)
 [10] Y. Liu, M. Davanço, V. Aksyuk, and K. Srinivasan, *Physical Review Letters* **110**, 223603 (May 2013)
 [11] S. McGee, D. Meiser, C. Regal, K. Lehnert, and M. Hol-

land, *Physical Review A* **87**, 053818 (2013)
 [12] S. Barzanjeh, M. Abdi, G. Milburn, P. Tombesi, and D. Vitali, *Physical Review Letters* **109**, 130503 (2012)
 [13] L. Tian, *Physical Review Letters* **110**, 233602 (2013)
 [14] Y.-D. Wang and A. A. Clerk, *Physical Review Letters* **110**, 253601 (2013)
 [15] S. Barzanjeh, D. Vitali, P. Tombesi, and G. Milburn, *Physical Review A* **84**, 042342 (2011)
 [16] S. Gröblacher, K. Hammerer, M. R. Vanner, and M. Aspelmeyer, *Nature* **460**, 724 (2009)
 [17] J. Teufel, D. Li, M. Allman, K. Cicak, A. Sirois, J. Whittaker, and R. Simmonds, *Nature* **471**, 204 (2011)
 [18] E. Verhagen, S. Deléglise, S. Weis, A. Schliesser, and T. J. Kippenberg, *Nature* **482**, 63 (2012)
 [19] A. Sørensen and K. Mølmer, *Physical Review Letters* **82**, 1971 (1999)
 [20] C. Sackett, D. Kielpinski, B. King, C. Langer, V. Meyer, C. Myatt, M. Rowe, Q. Turchette, W. Itano, D. Wineland, *et al.*, *Nature* **404**, 256 (2000)
 [21] A. Sørensen and K. Mølmer, *Physical Review A* **62**, 22311 (2000)
 [22] F. Massel, S. U. Cho, J.-M. Pirkkalainen, P. J. Hakonen, T. T. Heikkilä, and M. A. Sillanpää, *Nature Communications* **3**, 987 (2012)
 [23] V. Fiore, C. Dong, M. C. Kuzyk, and H. Wang, *Physical Review A* **87**, 023812 (2013)
 [24] T. Palomaki, J. Harlow, J. Teufel, R. Simmonds, and K. Lehnert, *Nature* **495**, 210 (2013)
 [25] S. Weis, R. Rivière, S. Deléglise, E. Gavartin, O. Arcizet, A. Schliesser, and T. J. Kippenberg, *Science* **330**, 1520 (2010)
 [26] A. H. Safavi-Naeini, T. M. Alegre, J. Chan, M. Eichenfield, M. Winger, Q. Lin, J. T. Hill, D. Chang, and O. Painter, *Nature* **472**, 69 (2011)
 [27] S. Mancini, V. Giovannetti, D. Vitali, and P. Tombesi, *Physical Review Letters* **88**, 120401 (2002)
 [28] M. Paternostro, D. Vitali, S. Gigan, M. Kim, C. Brukner, J. Eisert, and M. Aspelmeyer, *Physical Review Letters* **99**, 250401 (2007)
 [29] S. G. Hofer, W. Wicczorek, M. Aspelmeyer, and K. Hammerer, *Physical Review A* **84**, 052327 (2011)
 [30] H. Tan, G. Li, and P. Meystre, *Physical Review A* **87**, 033829 (2013)
 [31] M. J. Woolley and C. A. A, *Physical Review A* **87**, 063846 (2013)
 [32] A. Furusawa, J. L. Sørensen, S. L. Braunstein, C. A. Fuchs, H. J. Kimble, and E. S. Polzik, *Science* **282**, 706 (1998)
 [33] G. J. Milburn, arXiv preprint quant-ph/9908037(1999)
 [34] C. Genes, A. Mari, P. Tombesi, and D. Vitali, *Physical Review A* **78**, 032316 (2008)
 [35] M. B. Plenio, *Physical Review Letters* **95**, 090503 (2005)
 [36] G. Vidal and R. F. Werner, arXiv preprint quant-ph/0102117(2001)
 [37] K. Blow, R. Loudon, S. J. Phoenix, and T. Shepherd, *Physical Review A* **42**, 4102 (1990)
 [38] G. Vidal, *Journal of Modern Optics* **47**, 355 (2000)
 [39] S. Van Enk, *Physical Review A* **67**, 022303 (2003)

Supplementary Materials

Mark C. Kuzyk,* Steven J. van Enk, and Hailin Wang

Department of Physics and Oregon Center for Optics, University of Oregon, Eugene, OR 97403, USA

UNITARY EVOLUTION

In this section we discuss the evolution of the three-mode optomechanical system, neglecting all damping terms. The interaction Hamiltonian for the system is

$$H_I = (g_1 a_1 + g_2 a_2^\dagger) b^\dagger e^{i\Delta t} + \text{H.c.} \quad (1)$$

We assume from now on that the optomechanical coupling rates for the two optical modes are set equal, $g_1 = g_2 \equiv g$. We define dimensionless quadrature variables $x_i = (a_i + a_i^\dagger)/\sqrt{2}$, $x_b = (b + b^\dagger)/\sqrt{2}$, $p_i = i(a_i^\dagger - a_i)/\sqrt{2}$, and $p_b = i(b^\dagger - b)/\sqrt{2}$. From the optical field quadratures, we define two EPR variables $x \equiv x_1 + x_2$, and $p \equiv p_2 - p_1$, which satisfy $[x, p] = 0$ and can therefore be treated as numbers for the current treatment. In terms of these variables, the interaction Hamiltonian can be written in the form

$$H_I = f(t)x_b + g(t)p_b. \quad (2)$$

The time-dependent coefficients of the mechanical degrees of freedom are

$$f(t) = g[x \cos(\Delta t) + p \sin(\Delta t)] \quad (3)$$

$$g(t) = g[x \sin(\Delta t) - p \cos(\Delta t)]. \quad (4)$$

We write the exact propagator by ansatz, assuming the form

$$U(t) = e^{-iA(t)} e^{-iF(t)x_b} e^{-iG(t)p_b}, \quad (5)$$

and solve for the functions $A(t)$, $F(t)$, and $G(t)$ by enforcing that $U(t)$ satisfy the equation

$$i \frac{d}{dt} U(t) = H_I U(t). \quad (6)$$

In doing so, one finds the the solutions

$$F(t) = \int_0^t dt' f(t')$$

$$G(t) = \int_0^t dt' g(t') \quad (7)$$

$$A(t) = - \int_0^t dt' F(t') g(t')$$

Following through the integration yields

$$\begin{aligned} F(t) &= \frac{g}{\Delta} [x \sin(\Delta t) - p \cos(\Delta t) + p] \\ G(t) &= \frac{g}{\Delta} [x - x \cos(\Delta t) - p \sin(\Delta t)] \end{aligned} \quad (8)$$

and

$$\begin{aligned} A(t) &= - \frac{g^2}{\Delta^2} \left(\frac{t\Delta}{2} (x^2 + p^2) \right. \\ &\quad \left. + \frac{1}{4} \sin(2\Delta t) (p^2 - x^2) + \frac{px}{2} [\cos(2\Delta t) - 1] \right. \\ &\quad \left. - px [\cos(\Delta t) - 1] - p^2 \sin(\Delta t) \right). \end{aligned} \quad (9)$$

The coefficients of the mechanical degrees of freedom oscillate in time, simultaneously returning to zero whenever the timing condition $t_n = 2\pi n/\Delta$ for integer n is satisfied. At those times, the remaining part of the propagator entangles the optical modes with the operation of

$$A(t_n) = - \frac{g^2}{\Delta^2} \pi n (x^2 + p^2). \quad (10)$$

For optical states initially in the vacuum, the covariance matrix of the optical modes can be constructed, and a detailed calculation gives the logarithmic negativity

$$E_{\mathcal{N}} = -\frac{1}{2} \log_2 \left(2r^2 - \sqrt{4r^8 + 8r^6 + 5r^4 + r^2} + 2r^4 + \frac{1}{4} \right) - 1 \quad (11)$$

where $r = \pi n g^2 / \Delta^2$.

LOGARITHMIC NEGATIVITY

To quantify the entanglement between the optical modes of the system, we use the logarithmic negativity. For two-mode Gaussian states described by annihilation operators a_i ($i = 1, 2$) that satisfy the bosonic commutation relations $[a_i, a_j^\dagger] = \delta_{ij}$, the logarithmic negativity can be calculated from the expression

$$E_{\mathcal{N}} = \max(0, -\log_2 2\eta^-), \quad (12)$$

where

$$\eta^- = \frac{1}{\sqrt{2}} \sqrt{\Sigma - \sqrt{\Sigma^2 - 4 \det V}}, \quad (13)$$

and

$$\Sigma = \det A + \det B - 2 \det C. \quad (14)$$

The matrices A , B , and C are 2×2 blocks of the covariance matrix

$$V = \begin{pmatrix} A & C \\ C^\text{T} & B \end{pmatrix}. \quad (15)$$

The components of the covariance matrix have the usual form

$$V_{ij} = \frac{1}{2} \langle \Delta \xi_i \Delta \xi_j + \Delta \xi_j \Delta \xi_i \rangle, \quad (16)$$

where $\Delta \xi_i = \xi_i - \langle \xi_i \rangle$, and $\vec{\xi} = [x_1, p_1, x_2, p_2]^T$. The dimensionless quadrature variables x_i and p_i are constructed from the annihilation operators according to $x_i = (a_i + a_i^\dagger)/\sqrt{2}$ and $p_i = i(a_i^\dagger - a_i)/\sqrt{2}$.

From Eq. (12), one finds that the system becomes

entangled when $\eta^- < 1/2$. In terms of the covariance matrix, the requirement for entanglement is $4 \det V < \Sigma - 1/4$, which is equivalent to Simon's partial transpose criterion [?].

* Electronic address: mkuzyk@uoregon.edu